View metadata, citation and similar papers at core.ac.uk

brought to you by CORE

provided by NASA Technical Reports Server

3 1176 00165 9474

NASA CR-164,633

NASA-CR-164633
19810019935

COLLEGE OF ENGINEERING

VPI-E-80-8

February, 1980

Convergence Rates for Finite Element Problems with Singularities

Part I - Antiplane Shear

Robert Plunkett[1]

VIRGINIA POLYTECHNIC INSTITUTE AND STATE UNIVERSITY

BLACKSBURG, VIRGINIA

NF01144

NASA CR-164,633

College of Engineering
Virginia Polytechnic Institute and State University
Blacksburg, VA. 24061

VPI-E-80-8 February, 1980

Convergence Rates for Finite Element Problems with Singularities

Part I - Antiplane Shear

Robert Plunkett[1]

Department of Engineering Science and Mechanics

Interim Report 18 - NASA Grant CA #NCCI-15

Prepared for: Materials Application Branch
National Aeronautics & Space Administration
Langley Research Center
Hampton, VA. 23665

[1]Visiting Professor
Affiliation - Aerospace and Engineering Mechanics
University of Minnesota

N81-28473#

ABSTRACT

The finite element method is widely used to find the stress fields caused by external loads and temperature changes in composite materials. This report presents the first of a set of systematic studies of the rate of convergence and effect of singularities on such solutions. The problem considered is that of a finite crack in an infinite medium under anti-plane shear load. For this problem, it is shown that the nodal force at the trip of the crack accurately gives the order of the singularity, that energy release methods can give the strength to better than 1% with element size 1/10 the crack length and that nodal forces give a much better estimate of the stress field than do the elements themselves.

This study is being extended to inplane shear, uniform tension and composite materials as well as finite bodies of rectangular form.

TABLE OF CONTENTS

		Page
ACKNOWLEDGEMENTS		iii
SECTION I.	INTRODUCTION	1
II.	NUMERICAL SOLUTION	2
III.	RESULTS	4
IV.	CONCLUSIONS	5
APPENDIX I.	FINITE ELEMENT FORMULATION	9
II.	FACTORING TRIDIAGONAL MATRICES	14
REFERENCES		16
FIGURE 1a	Stress fields	18
1b	Nodal force convergence	18
2	Singularity-convergence vs. element size	19
TABLE I		20

ACKNOWLEDGEMENTS

This work was accomplished during a sabbatical leave at VPI & SU with financial support from VPI & SU and the University of Minnesota. The author has benefitted greatly from conversations with Profs. C. T. Herakovich, J. L. Jenkins, M. P. Kamat and C. W. Smith.

I. INTRODUCTION

The finite element method is widely used to find stress fields in non-homogeneous elastic materials, such as composites. For fracture analysis the most important information is usually the strength and nature of the singularity at the tip of a crack or at an interface between two laminae [e.g., 1,2]. Since the stress and strain fields are non-analytic at such singularities, it is difficult to improve the accuracy by the accepted procedure of averaging the stress or strain values in contiguous elements [3]. Pian and Tong [4] have shown that a minimum potential energy formulation gives nodal displacements which converge uniformly to the continuum solution for the displacement field. They and Perks [5,6] have discussed the convergence to the stress field in the vicinity of a singularity. The current method of choice is to fit the stress field near the tip by a region with a very fine mesh [7] or by using a special singular element [7,8]. The first method requires a large number of points and the second requires a prior knowledge of the nature of the singularity.

From Pian's work, it would appear that more information can be had from the nodal forces than has so far been exploited for static solutions; some work has already been done on finding energy release rates for both dynamic [9,10] and static problems [11,14].

A finite crack in an infinite elastic solid loaded at infinity in tension (Type I), plane shear (Type II) or antiplane shear (Type III) are useful subjects for investigation of convergence because they are conveniently modeled with rectangular elements, the resulting matrix equations may be solved with difference equation techniques, and the

solutions are well known for the homogeneous case. This report gives extensive results for antiplane shear; work continues on the other two loadings and on laminates.

II. NUMERICAL SOLUTION

A finite element solution for strain field in an infinite solid with an infinite plane crack of width 2c subjected to uniform antiplane shear at infinity is a set of nodal displacements $w_{i,j}$ with the indices i,j going from $-\infty$ to $+\infty$. If we put i = j = 0 at the center of the crack, then $w_{-i,j} = -w_{i,j}$ and $w_{i,-j} = w_{i,j}$ so that we only need the solution for non-negative i and j. Solution details are given in Appendix I where it is shown that, for the residual problem, the nodal forces on the crack are $f_{oj} = -1$, $-N < j < +N$ and the displacements $w_{oj} = 0$, $|N| \leq |j|$. We intend to investigate the effect of mesh size on the convergence of the solution; to do so, it is convenient to convert the above problem into the finite equivalent of a boundary integral problem by finding the finite equivalent of the Green's Function (N = 1) and then using superposition.

Pian shows [4] that the displacement field defined by the nodal displacements and linear or bilinear element displacement fields (Appendix I) gives a total potential energy greater than that in the continuum if the boundary nodes are loaded by forces equal to

$$F_{oj} = \int_{j-1}^{j+1} w(\xi)\tau(\xi)d\xi \qquad (1)$$

where $w(\xi)$ is the (linearly varying) constrained displacement field.

For this to be valid, we must use the force boundary conditions of equation I-13b. In Appendix I, it is shown that the residual problem has a constant shear stress on the crack, so that the elements of f_o are all -1. We get the solution in two steps; the first step is to find the displacement field for $w_{oo} = 1$, $w_{oj} = 0$, $j \neq 0$. From equations I-14 and I-17 in Appendix I:

$$w_{1j} = \frac{1}{N}\left[c_o/2 + \sum_{j=1}^{N-1} c_j \cos(jk\pi/N) + (-1)^j c_N/2\right] \tag{2}$$

If we now let $N \to \infty$

$$w_{1j} = \int_0^1 c(\xi)\, \cos\pi j\xi \, d\xi \tag{3}$$

where $k\pi/N \to \pi\xi$ in equations I-16 and II-4. From equation II-2, it can be seen that

$$w_{ij} = \int_0^1 c^i(\xi)\, \cos\pi j\xi \, d\xi \tag{3}$$

so that the nodal displacement field can be found by numerical integration; we only need w_{1j} for our work. f_{oo} is now found from equation I-6 or I-7; if we divide each element of $\tilde{w}_1$ by f_{oo} we have the first row of the displacement field for a unit force at i=0,j=0 and f_o is found from equation I-13b. The linear (triangular element) and bilinear (rectangular) element values for $f_{o,200}$ agreed within 4×10^{-10} (0.01%) and agreed with the continuum value for $\tau_{yz} - 1$ (Equation I-3) within 5×10^{-9}.

For crack length of 2N elements, we may write:

$$D_1 \tilde{w}_o^{(2N)} = f_o^{(2N)} \tag{4}$$

where $f_o^{(2N)}$ is a column of 1's, 2N-1 long and D_1 is a (2N-1)x(2N-1) matrix each row of which is $\tilde{f}_o^{(2)}$, found from equation I-13b, with the f_{oo} term on the main diagonal. Equation 4 can be reduced to N equations, since $w_{oj} = w_{o,-j}$, and solved for $\tilde{w}_o$. The nodal forces for $N \leq j$ are now found by extending D_1 into D_2 and writing

$$D_2 \tilde{w}_o^{(2N)} = \hat{f}_o$$

where the elements of $\hat{f}_o$ are $f_{o,j}$, $j \geq N$.

III. RESULTS

Using the bilinear rectangular elements, the nodal force at j = N+1 is about 7.5% lower than τ/τ_o at x = N/N+1. For a constant x, this error decreases almost linearly with 1/N so that linear extrapolation gives remarkably accurate results. For example, the finite element value for x = 1.25 c is 1.5962 for the 8 element solution and 1.6302 for 16. Linear extrapolation to 1/M = 0 gives 1.6643; the continuum value is 1.6667, an error of 0.14%. Figure 1A shows τ_{yz}/τ_o vs r/c as given by equations I-3 and I-4. It would be difficult to distinguish the finite element values from the exact curve for j > N+1 but F_{N+1} is shown for N from 2 to 64. The trend for the constant strain (linear) elements is about the same but with about twice the error.

The above comparison shows, as is well known, that the nodal displacement values converge to the continuous displacement function at a rate appropriate to the order of the equivalent finite difference algorithm and that the stresses at any analytic point may be found by numerical differentiation of the displacement field to the same order

by using Hooke's law. Averaging the "stresses" in contiguous constant strain elements gives less accurate values unless the weighting points are carefully selected, e.g., the Gaussian integration points [3].

One would expect [4] the singular force at j = N to be given by the weighted integral of the stresses on the y = 0 face from j = N-1 to N+1. If we consider the original (not the residual) problem, $\tau = 0$, $j < N$. Then using equation I-3 and a linear weighting function

$$F_N = \frac{1}{h}\int_1^{1+h} \frac{x(1 - x/h)}{\sqrt{x^2 - 1}}\, dx$$

$$= \frac{\sqrt{8h}}{3}\,(1 + o(h))$$

$$= 0.9428\,\sqrt{h}$$

where $h = 1/N$. The continuum residual problem converted to finite element form differs from the residual finite element problem by adding 0.5 h to F_N.

Since the displacement field solution is not analytic at the singularity, equations I-9 and I-11 don't apply. However, we are integrating only on a line where w = o and $\frac{\partial^2 w}{\partial x^2} = 0$ so that we may let $w_{oj} = 0$ in these equations; if we use only $w_{1,N-1}$, $w_{1,N}$ and $w_{1,N+1}$ we should get $\frac{\partial w}{\partial y}$, $o(h^4)$. These and several other less accurate ($o(h^2)$) approximations were used and they all converged very rapidly to $c_1\sqrt{h}$. The points for the bilinear case are shown in Figure 1b. Rather than attempting to find the slope from the log-log plot, it is better to extrapolate $F_N/\sqrt{h}$ vs h to h = 0. These curves are shown in figure 2 where we compare the nodal force at i = 0, j = N using equation I-11 modified by letting $w_{o,j} \equiv 0$, the linear approximation for $\frac{\partial w}{\partial y}$ and the second order approximation in which

we use $\frac{\partial^2 w}{\partial x^2} + \frac{\partial^2 w}{\partial y^2} = 0$. These algorithms are:

$$F_N = -\frac{1}{3}(w_{1,N-1} + w_{1,N} + w_{1,N+1}) \text{ (Eq I-11 mod)} \tag{5}$$

$$F_N = w_{1,N} = \frac{\partial w}{\partial y} + o(h^2) \tag{6}$$

$$F_N = -\frac{1}{6}(w_{1,N-1} + 4w_{1,N} + w_{1,N+1}) = \frac{\partial w}{\partial y} + o(h^4) \tag{7}$$

All of the curves converge to a square root singularity but the bilinear ones do so in a linear fashion which makes extrapolation accurate for crack lengths as coarse as 16 elements (N = 8). Unfortunately, they don't extrapolate to the correct coefficient, which shows that higher order terms must be included even in the limit. Table I shows the rate of convergence for F_N to its value at h = 0 using equation 7 for both the linear and bilinear case and to the square root singularity for equations 6 and 7.

The external work done is another measure of the strength of the singularity. The external work, equal to the strain energy, is

$$\pi/2 = U(c = 1) = \int_{-1}^{1} w(x)\tau_{yz}(x)dx$$

$$\approx \frac{1}{N^2} \sum_{j=-(N-1)}^{N-1} w_{oj}(x) \text{ or Simpson's} \tag{8}$$

because $F_j = 1$. As shown in Table 1, this converges as rapidly as F_N, and converges to the correct value. The columns headed δ are the result of linear extrapolation using the entry and the previous entry; thus the extrapolation of U from the bilinear solution using 2 and 4 elements for the half crack length gives $\pi/4$ with an error of 0.3%. One may also approximate the energy release rate from $2 \cdot (w_{N\cdot 1} \cdot F_N/2)$. This should

converge to

$$\frac{dU}{dc} = \pi c \tag{9}$$

The % error for the linear and bilinear case and for the extrapolated values are shown in the last four columns of Table I. These results are better than Rybicki [14] indicates.

Since the values for $w_{o,50}^{(2)}$ agreed within 5×10^{-8} in the linear and bilinear cases and the small table top computer used in this work took about one minute per integration (equation 3), the values for $j > 50$ from the linear case were used for the bilinear solutions. This small inconsistency accounts for the non-uniform convergence at levels of 10^{-4} for N = 64 in Table I.

IV. CONCLUSIONS

It has been shown that the singularity at a crack tip under antiplane shear (Type III) can be accurately modeled with a relatively coarse mesh near the tip if one uses the energy release from crack extension. The results are remarkably accurate if one gets solutions for two or three element sizes and extrapolates to zero size (Table I).

Curve fitting to the stress field requires a very fine mesh both because the slope of the continuum solution departs rapidly from that of the leading term and because the finite element solution is oscillating at the first two or three nodal points (see also Wilson [7]).

The nodal force at the crack tip as a function of mesh size is a very accurate measure of the order of the singularity but may converge to the wrong strength if higher order terms are not included. Even

where the displacement field is analytic, the nodal forces give a better approximation to the stress field than does element averaging.

The methods used in this report are being extended to Types I and II loading and laminated material and could be used for finite bodies of rectangular shape. They are economical with computer time since by using boundary element techniques, only small matrices need be inverted to get finite element solutions for large (or infinite) arrays. The results presented here were obtained on a small (64K bytes) table top computer.

APPENDIX I - FINITE ELEMENT PROBLEM FORMULATION

Our problem is that of a crack of length $-c \leq x \leq c$ in the $y = 0$ plane, extending to $\pm \infty$ in the z direction of the infinite solid with a uniform shear stress $\tau_{yz} = \tau_o$ at $x^2 + y^2 \to \infty$ (antiplane, Type III). This is the same problem as the edge crack of length c in the semi-infinite solid, $x \geq 0$. The continuum solution is given by Bentham and Koiter [12, Sect 3.3]. For antiplane shear:

$$\left.\begin{aligned} &\tau_{xz} - \tilde{i}\,\tau_{yz} = 2\phi'(\zeta) \\ &\zeta = x + \tilde{i}y \\ &Gw = \phi(\zeta) + \overline{\phi}(\zeta) \\ &\tilde{i} = \sqrt{-1} \end{aligned}\right\} \qquad \text{I-1}$$

For our geometry:

$$\phi(\zeta) = -\frac{1}{2}\,\tilde{i}\,\tau_o\,(\zeta^2 - c^2)^{1/2} \qquad \text{I-2}$$

Along the x axis

$$\tau_{yz} = \tau_o \left(\frac{x^2}{x^2 - c^2}\right)^{1/2} \qquad x^2 > c^2 \qquad \text{I-3}$$

There is a singularity of order 1/2 at $x^2 = c^2$. For $\quad > 0$, let

$$\left.\begin{aligned} &x = c + r \quad , \quad \alpha = \frac{r}{c} \\ \text{Then} \quad &\tau_{yz} = \tau_o (2\alpha)^{-1/2}\left(1 + \frac{3}{4}\,\alpha + o(\alpha^2)\right) \\ \text{and} \quad &K_{III} = \tau_o\, c^{1/2} \end{aligned}\right\} \qquad \text{I-4}$$

The finite element problem is more easily handled if we subtract a uniform stress field from the above, leaving a boundary condition of:

$$\left.\begin{aligned} \tau_{yz} &= -\tau_o \qquad y = 0 \quad , \quad x^2 < c^2 \\ \tau &\to 0 \qquad x^2 + y^2 \to \infty \end{aligned}\right\} \qquad \text{I-5}$$

We use a square grid of nodal points at x = j, y = i subjected to a shear stress $\tau = 1$ on the negative face $i = 0$, $-c < j < c$ and let $G = 1$. By symmetry:

$$w_{-i,j} = -w_{i,j}$$

$$w_{i,-j} = w_{i,j}$$

The basic element is the square of side 1. By minimizing the strain energy [3] we can show that the nodal force at point i,j of the element(s) bounded by i, i+1, j and j+1 is:

$$\tilde{F}_{ij} = w_{ij} - \frac{1}{2} w_{i+1,j} - \frac{1}{2} w_{i,j+1} \qquad \text{I-6}$$

for a uniform strain field in the two triangular elements bounded either by the line (i,j)(i+1,j+1) or (i+1,j)(i,j+1). It is interesting and useful that for antiplane shear the direction of the diagonal does not affect equation I-6. For the bilinear displacement field:

$$w = w_{ij}\,(1-\zeta)(1-\eta) + w_{i+1,j}\,\zeta(1-\eta)$$

$$+ w_{i,j+1}(1-\zeta)\eta + w_{i+1,j+1}\,\zeta\eta$$

the corresponding equation is:

$$\tilde{F}_{ij} = \frac{2}{3} w_{ij} - \frac{1}{6} w_{i+1,j} - \frac{1}{6} w_{i,j+1} - \frac{1}{3} w_{i+1,j+1} \qquad \text{I-7}$$

These elements are now assembled to give a zero nodal force for $i \neq 0$. Using equation I-6 the field equations are

$$F_{ij} = 0 = -w_{i-1,j} - w_{i,j-1} + 4w_{i,j} - w_{i,j+1} - w_{i+1,j} \qquad \text{I-8}$$

and the nodal force on the negative y face is

$$F_{ij}^{-} = -\frac{1}{2} w_{i,j-1} + 2w_{i,j} - \frac{1}{2} w_{i,j+1} - w_{i+1,j} \qquad \text{I-9}$$

Using equation I-7, they are

$$\begin{aligned} 0 = &-\frac{1}{3}(w_{i,j-1} + w_{i-1,j} + w_{i-1,j+1}) \\ &+ (-\frac{1}{3} w_{i,j-1} + \frac{8}{3} w_{i,j} - \frac{1}{3} w_{i,j+1}) \\ &- \frac{1}{3}(w_{i+1,j-1} + w_{i+1,j} + w_{i+1,j+1}) \end{aligned} \qquad \text{I-10}$$

and

$$\begin{aligned} F_{ij}^{-} = &-\frac{1}{3}(w_{i-1,j-1} + w_{i-1,j} + w_{i-1,j+1}) \\ &+ \frac{1}{2}(-\frac{1}{3} w_{i,j-1} + \frac{8}{3} w_{i,j} - \frac{1}{3} w_{i,j+1}) \end{aligned} \qquad \text{I-11}$$

Equation I-8 is the finite difference equation for the Laplacian good to $o(h^2)$; using the governing partial differential equation

$$\frac{\partial^2 w}{\partial x^2} + \frac{\partial^2 w}{\partial y^2} = 0 \qquad \text{I-12}$$

we find that equation I-9 gives the first derivative, w_y, $o(h^2)$, while $w_{i,j} - w_{i+1,j}$ is $o(h)$. Normally we can use $\frac{1}{2}(w_{i-1,j} - w_{i+1,j})$ which is $o(h^2)$ but not at a stressed surface. This same result does not hold for equations I-10 and 11 but we can show that the system converges $o(h^4)$.

The corresponding matrix equation is

$$-B\tilde{w}_{i-1} + A\tilde{w}_i - B\tilde{w}_{i+1} = 0 \qquad \text{I-13a}$$

$$E\tilde{w}_0 - F\tilde{w}_1 = \frac{1}{2} A\tilde{w}_0 - B\tilde{w}_1 = \tilde{f}_0 \qquad \text{I-13b}$$

where $\tilde{w}_i$ is the column vector of the displacements of the nodes in i^{th} row. Using the notation of Appendix II, the values of a and b in equation II-1 are those in Table I.

Equation	I-8		I-9		I-10		I-11	
Matrix	A	B	E	F	A	B	E	F
a	4	-1	2	-1	8/3	-1/3	4/3	-1/3
b	-1	0	-1/2	0	-1/3	-1/3	-1/6	-1/3

Table I-1

We may solve the matrix difference equation I-13a, by expanding $\tilde{w}_i$ in the eigenvectors of Appendix II. Using equation II-7, if we substitute:

$$\left.\begin{aligned} \tilde{w}_i &= \underline{\overline{X}}\, \tilde{q}_i \\ A &= \underline{\overline{X}}\, \Lambda_A\, \underline{\overline{Y}} \\ B &= \underline{\overline{X}}\, \Lambda_B\, \underline{\overline{Y}} \end{aligned}\right\} \qquad \text{I-14}$$

into equation I-13a and use the last of equations II-2, the equations for $\tilde{q}_i$ are decoupled:

$$-\Lambda_B\, \tilde{q}_{i-1} + \Lambda_A\, \tilde{q}_i - \Lambda_B\, \tilde{q}_{i+1} = 0 \qquad \text{I-15}$$

If we now let:

$$\left.\begin{aligned} q_{ik} &= c_k\, q_{i-1,k} \\ \text{then} \quad -\lambda_{Bk}\, c_k^{-1} + \lambda_{Ak} - \lambda_{Bk}\, c_k &= 0 \\ \text{and} \quad c_k &= \beta_k \pm \sqrt{\beta_k^2 - 1} \\ \text{where} \quad \beta_k &= \lambda_{Ak}/2\lambda_{Bk} \end{aligned}\right\} \qquad \text{I-16}$$

λ_{Ak} and λ_{Bk} are given by equation II-4 and a and b are shown in table I-1. In order to satisfy the condition at infinity, we take the + or - sign to make $c^2 < 1$. $c_k \to 1/2\ \beta$ as $\beta^{-1} \to 0$.

If $w_{oo} = 1$, $w_{oj} = 0$, $j \neq 0$, from equations I-13a and I-16

$$\lambda_{Ak}\, q_{ik} - \lambda_{Bk}\, q_{2k} = \lambda_{Bk}\, \chi_{ok}\, w_{oo} = \lambda_{Bk}\, w_{oo}$$

$$(\lambda_{Ak} - c\, \lambda_{Bk})\, q_{ik} = \lambda_{Bk}\, w_{oo}$$

or

$$q_{ik} = c_k\, w_{oo} \qquad \text{I-17}$$

APPENDIX II - FACTORING TRIDIAGONAL MATRICES

The matrices we are concerned with all have one constant, a, on the main diagonal and another, b, on the first sub and superdiagonal with all other elements zero. By symmetry, they extend from -N to +N and are (2N+1) x (2N+1) square. In order to get symmetrical reflection at ± N, we make the second element of the first row and the next to the last element of the last row equal to 2b which gives the following form.

$$R = \begin{bmatrix} a & 2b & 0 & 0 & . & . & . \\ b & a & b & 0 & . & . & . \\ 0 & b & a & b & . & . & . \\ \cdots & \cdots & \cdots & \cdots & \cdots & \cdots & \cdots \\ & 0 & b & a & b & 0 & \\ . & . & . & . & . & . & . \\ . & . & . & . & . & . & . \\ . & . & . & . & 0 & 2b & a \end{bmatrix} \qquad \text{II-1}$$

The associated eigenvalue problem is:

$$\left.\begin{aligned} R\overline{X} &= \overline{X}\Lambda \\ \overline{Y}R &= \Lambda\overline{Y} \\ \text{normalized to} \quad \overline{Y}\,\overline{X} &= I \\ \text{so that} \quad R = \overline{X}\Lambda\overline{Y} \quad &\text{and} \quad \overline{Y}R\overline{X} = \Lambda \end{aligned}\right\} \qquad \text{II-2}$$

where Λ is the diagonal matrix of the eigenvalues, $\overline{X}$ is the square matrix of the eigenvector columns and $\overline{Y}$ is the adjoint square matrix of the eigenvector rows. The difference equations are:

$$\left.\begin{aligned} b\,x_{i-1,k} + a\,x_{i,k} + b\,x_{i+1,k} &= \lambda_k\,x_{i,k} \\ a\,x_{-N,k} + 2b\,x_{-N+1,k} &= \lambda_k\,x_{-N,k} \\ 2b\,x_{N-1,k} + a\,x_{N,k} &= \lambda_k\,x_{N,k} \end{aligned}\right\} \qquad \text{II-3}$$

The matrix has 2N+1 roots:

$$\lambda_k = a + 2b \cos (k\pi/2N) \qquad k = 0,1,\ldots,2N+1 \qquad \text{II-4}$$

The corresponding column eigenvectors are:

$$\chi_{ik} = \cos (ik/2N) \qquad i = -N,\ldots,0,\ldots,N \qquad \text{II-5}$$

The adjoint row eigenvectors are:

$$Y_{ki} = (1 - \tfrac{1}{2} \delta_{i,\pm N})(1 - \tfrac{1}{2} \delta_{\pm N,k})\chi_{ik}/N \qquad \text{II-6}$$

where δ_{ij} is the Kronecker δ.

The antisymmetric tridiagonal matrix found by replacing the 2b terms in equation II-1 with 0, has the same eigenvalues, but sines for the eigenvectors (equation II-5) instead of cosines.

REFERENCES

1. Herakovich, C. T., A. Nagarkar and D. A. O'Brien, "Failure Analysis of Composite Laminates with Free Edges," in Modern Development in Composite Materials and Structures, J. S. Vinson, ed. ASME, 53-66, 1979.

2. Reifsnider, K. L., "Mechanics of Failure of Composite Materials," Proc. Int'l. Symp. on Fracture Mech., ONR/GWU, Wash., D.C., 1978.

3. Zienkiewicz, O. C., "The Finite Element Method," McGraw-Hill (U.K.) 3rd ed., 1977.

4. Pian, T. H. H. and P. Tong, "Basis of Finite Element Methods for Solid Continua," Int. J. Num. Methods in Engineering, 1, 1, 3-28 (1969).

5. Tong, P. and T. H. H. Pian, "On the Convergence of the Finite Element Method for Problems with Singularity," Int. J. Solids and Structures, 9, 313-321 (1973).

6. Perkes, D. M., "On the Convergence of Finite Elements in the Presence of Singularities," Int. J. Num. Methods in Engineering, 14, 5, 780-784 (1979).

7. Wilson, W. K., "Finite Element Methods for Elastic Bodies Containing Cracks," in Methods of Analysis and Solutions of Crack Problems, G. L. Sih, ed., Noordhoff, 484-515, 1973.

8. Atluri, S. N., T. Nishioka and M. Nakagaki, "Numerical Modeling of Dynamic Crack Propagation by Moving Singular Elements," in Nonlinear and Dynamic Fracture Mechanics, N. Perrone and S. Atluri, eds., AMD-31, ASME, 37-66, 1979.

9. Caldis, E. S., D. R. J. Owen and O. C. Zienkiewicz, "Nonlinear Dynamic Transient Methods in Crack Propagation Studies," in AMD-31, ASME, 1-18 [see 8].

10. Kobayashi, A. S., "Dynamic Fracture Analysis by Dynamic Finite Method," in AMD-31, ASME, 19-36 [see 8].

11. Wang, A. S., F. W. Crossman and G. E. Law, "Interlaminar Failure in Epoxy Based Composite Laminates," in Advanced Composites: Design and Applications, T.R. Shives and W. A. Willord eds, NBS Spec. Pub. 563, Washington, D.C., 1979.

12. Bentham, J. P. and W. T. Koiter, "Asymptotic Approximations to Crack Problems," in Methods of Analysis and Solutions of Crack Problems, G. C. Sih, ed., Noordhoff, 131-178, 1973.

13. Abramovitz, M., and I. A. Stegun, "Handbook of Mathematical Functions," N.B.S. 1962 or Dover 1976.

14. Rybicki, E. F., and M. F. Kanninen, "Finite Element Calculation of Stress Intensity Factors by a Modified Crack Closure Integral," Eng. Fract. Mech., 9, 1977, pp. 931-38.

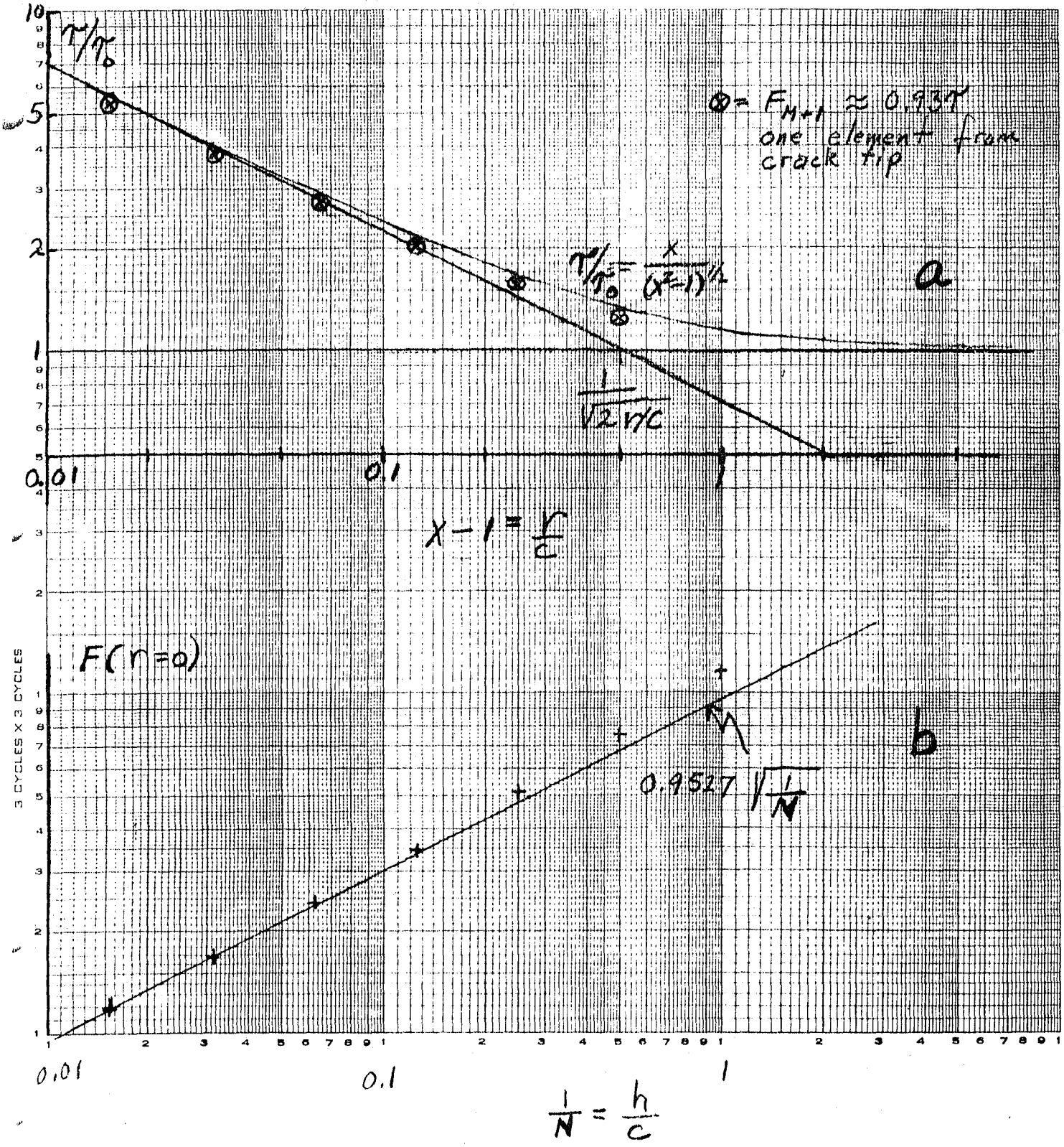

Figure 1a. Stress fields.

Figure 1b. Nodal force convergence.

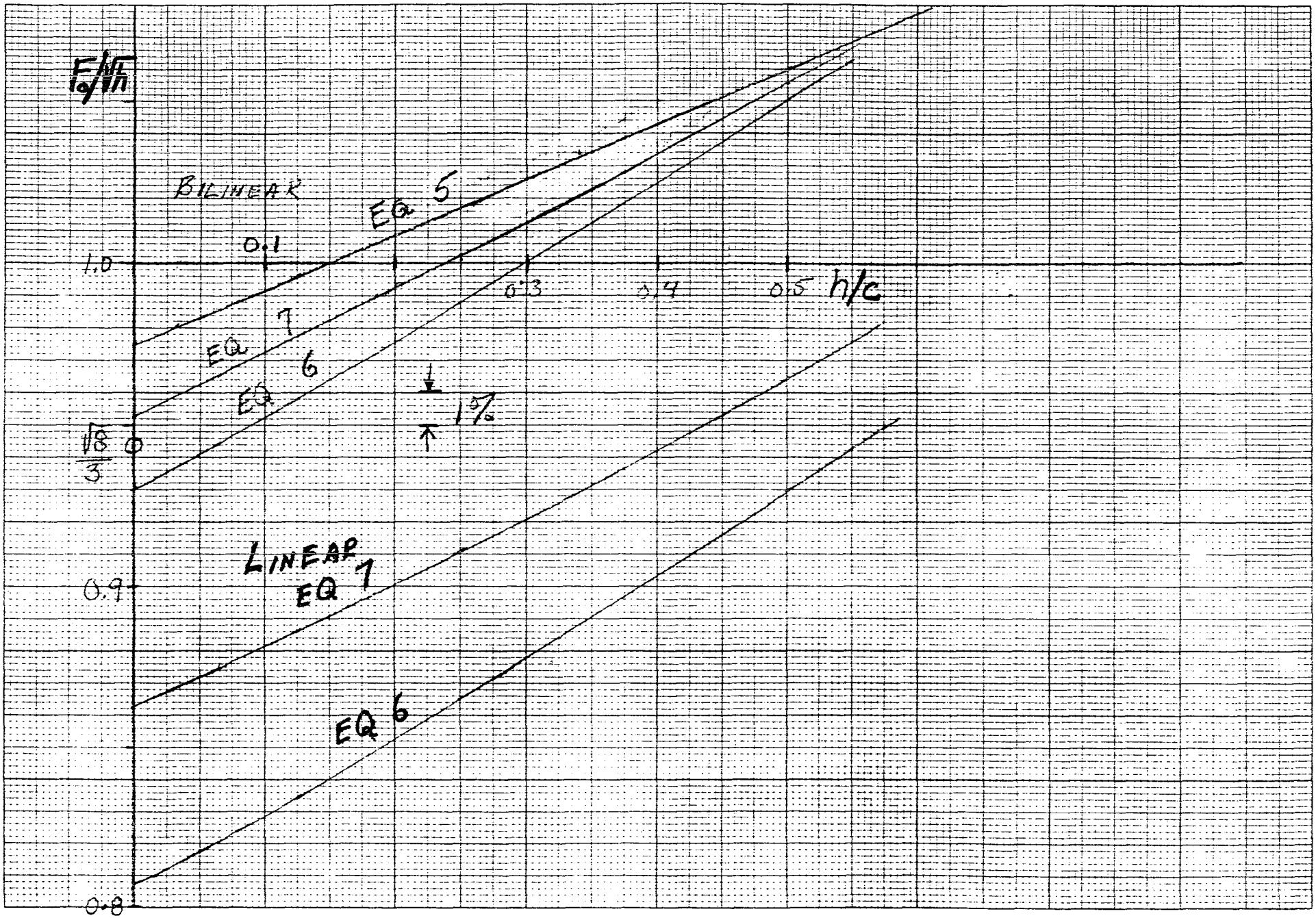

Figure 2. Singularity-convergence vs. element size.

FIGURE 2.

$$\% \text{ CONVERGENCE} = 100 \frac{|X_{oo} - X_M|}{X_{oo}}$$

c/h M	F_N (r = 0)		$\tau = r^{-\alpha}$ α		Bilinear		Bilinear		Linear		Bilinear		Linear	
	Bi $o(h)^4$	Linear $o(h)^4$	$o(h^4)$	δ	$o(h^2)$	δ	U	δ	U	δ	$F_N W_{N-1}$	δ	$F_N W_{N-1}$	δ
1	22.4	27.4	---	---	---	---	32	---	61	---				
2	10.8	11.8	28.5	---	34.3	---	21	10.2	33.4	6.0	11.9		19.9	
4	5.2	5.9	14.8	1.2	17.8	1.2	10.3	0.30	17.2	1.1	5.5	0.9	9.3	1.28
8	2.6	2.8	7.4	0.02	8.8	0.06	5.1	0.07	8.7	0.22	2.7	0.21	4.5	0.24
16	1.3	1.4	3.7	0.06	4.4	0.10	2.6	0.03	4.4	0.05	1.3	0.05	2.24	0.05
32	0.6	0.7	1.8	0.01	2.2	0.04	1.3	0.004	2.2	0.013	0.6	0.012	1.11	0.013
64	0.3	0.3	0.9	0.04*	1.1	0.03*	0.6	0.007*	1.1	0.004	0.3	0.018*	0.55	0.004
	(a)		(b)				(c)				(d)			

(a) linear $h \to 0$, $F_\infty = 0.953$ $\qquad \sqrt{8}/3 = 0.943$

(b) linear $h \to 0$, $F_\infty = 0.862$

(c) $U_\infty = \pi/2$, $\alpha_\infty = 1/2$

(d) $F_N W_{N-1} \to \pi/2N$

* Inaccurate to 10^{-4}

TABLE I

Prof. Donald F. Adams
Dept. Of Mechanical Engineering
University Of Wyoming
Larmie, WY 82070

Dr. N. R. Adsit
General Dynamics Convair
P.O. Box 80837
San Diego, CA. 92138

Dr. J. A. Bailie
D81-12 Bldg. 154
Lockheed Missiles & Space Co,Inc
1111 Lockheed Way
Sunnyvale, CA. 94088

Mr. Henry W. Bergner, Jr.
The Boeing Company
Mail Stop 3707
Seattle, WA. 98124

Dr. Charles W. Bert, Director
School Of Aerospace, Mechanical
& Nuclear Engineering
The University Of Oklahoma
Norman, Oklahoma 73069

Mr. Richard Boitnott
Mail Stop 188a
Nasa-Langley Research Center
Blacksburg, Va. 24061

Mr. David Bowles
Mail Stop 188B
NASA-Langley Research Center
Hampton, Va. 23665

Dr. H. F. Brinson
ESM Dept.
VPI&SU
Blacksburg, VA. 24061

Dr. Micharl F. Card
Mail Stop 190
NASA-Langley Research Center
Hampton, VA 23665

Dr. C. Chamis
NASA-Lewis Research Center
2100 Brook Park Rd.
Cleveland, Ohio 44135

Dr. Paul A. Cooper
Mail Stop 190
NASA-Langley Research Center
Hampton, Va. 23665

Dr. Frank Crossman
Lockheed Research Lab
Org. 52-41, Bldg. 204
3251 Hanover Street
Palo Alto, CA. 94304

Dr. I. M. Daniel, Manager
IIT Research Institute
10 West 35 Street
Chicago, IL. 60616

Dr. John R. Davidson
Mail Code 188E
MD-Structural Integrity Branch
Langley Research Center
Hampton, VA. 23665

Dr. John G. Davis, Jr.
Mail Stop 188A
Langley Research Center
Hampton, VA. 23665

Mr. Jerry W. Deaton
Mail Stop 188A
NASA-Langley Research Center
Hampton, VA. 23665

Mr. H. Benson Dexter
Mail Stop 188A
NASA-Langley Research Center
Hampton, VA. 23665

Mr. O. Earl Dhonau
Section 2-53400
Vought Corp.
P.O. Box 5907
Dallas, TX. 75222

Dr. S. C. Dixon
Mail Stop 395
NASA-Langley Research Center
Hampton, VA. 23665

Dr. J. E. Duberg
Mail Stop 103
NASA-Langley Research Center
Hampton, Va. 23665

Dr. M. F. Duggan
52-33/205/2
Lockheed Palo Alto Lab.
3251 Hanover St.
Palo Alto, Ca. 94304

Dr. Wolf Elber
Mail Stop 188E
NASA-Langley Research Center
Hampton, VA. 23665

Mr. Gary L. Farley
Mail Stop 188A
NASA-Langley Research Center
Hampton, VA. 23665

Mr. Larry Fogg
Lockheed-California
Dept. 7572, Bldg. 63, Plant A1
P.O. Box 551
Burbank, CA. 91520

Dr. R. L. Foye
USAMRDL
SAUDLAS (207-5)
Moffet Field, CA. 94035

Dr. D. Frederick
ESM Dept.
VPI&SU
Blacksburg, VA. 24061

Mr. Samuel P. Garbo
McDonnell Aircraft Co.
Bldg. 34, Post 350
St. Louis, MO. 63166

Mr. Ramon Garica
Mail Stop 190
NASA-Langley Research Center
Hampton, VA. 23665

Dr. Login B. Greszczuk
McDonnell Douglas Astr. Co.
5301 Bolas Avenue
Huntington Beach, CA. 92647

Mr. Glen C. Grimes, Engr. Spec.
Structures R & T, Dept 3780/62
Northrop Corp., Aircraft Div.
3901 W. Broadway
Hawthorne, CA. 90250

Dr. H. T. Hahn
Washington University
St. Louis, MO. 63130

Dr. J. C. Halpin
Flight Dynamics Lab
Wright-Patterson AFB
Ohio 45433

Professor Z. Hashin
School of Engineering
Dept. of Solid Mech. Materials
and Structures
Tel Aviv University
Tel Aviv, Israel

Dr. R. A. Heller
ESM Dept.
VPI&SU
Blacksburg, VA. 24061

Dr. E. G. Henneke
ESM Dept.
VPI&SU
Blacksburg, VA. 24061

Professor Phil Hodge
107 Aeronautical Engr. Bldg.
University of Minnesota
Minneapolis, MN 55455

Dr. K. E. Hofer
IIT Research Institute
10 West 35 Street
Chicago, Illinois 60616

Mr. Edward L. Hoffman
Mail Stop 188A
NASA-Langley Research Center
Hampton, VA. 23665

Dr. Peter W. Hsu
Mail Stop 1-1-12
Hamilton Standard Division
Windsor Locks, CT. 06096

Mr. Edward A. Humphreys
Materials Science Corporation
Blue Bell Office Campus
Blue Bell, PA. 19422

Dr. Michael W. Hyer
ESM Dept.
VPI&SU
Blacksburg, VA. 24061

AVCO, Systems Division
Subsystems & Meth. Structures
201 Lowell Street
Wilmington, MA. 01887

Dr. Eric R. Johnson
ESM Dept.
VPI&SU
Blacksburg, VA. 24061

Dr. N. J. Johnson
Mail Stop 226
NASA-Langley Research Center
Hampton, VA. 23665

Dr. M. P. Kamat
ESM Dept.
VPI&SU
Blacksburg, VA. 24061

Dr. Keith T. Kedward
1768 Granite Hills Dr.
El Cajon, CA. 92021

Mr. John M. Kennedy
Mail Stop 188E
NASA-Langley Research Center
Hampton, VA. 23665

Mr. James F. Knauss
Section 2-30400
Vought Corp.
P.O. Box 225907
Dallas, TX. 75265

Dr. Ronald D. Kriz
Dept. Com. NBS Bldg. 2
Boulder, CO. 80302

Dr. S. V. Kulkarni
L342 Lawrence Livermore Lab
P. O. Box 808
Livermore, Ca. 94550

Dr. M. R. Louthan
Materials Engineering
VPI&SU
Blacksburg, VA. 24061

Mr. Vic Mazzio
General Electric Co.
P.O. Box 8555
Bldg. 100, Rm. M4018
Philadelphia, PA. 19101

Mr. Robert R. McWithey
Mail Stop 190
NASA-Langley Research Center
Hampton, VA. 23665

Dr. Martin M. Mikulas
Mail Stop 190
NASA-Langley Research Center
Hampton, VA. 23665

Mr. J. Steve Mills
6100 Edinger Ave., Apt. 525
Huntington Beach
CA 92647

Dr. D. H. Morris
ESM Dept.
VPI&SU
BLACKSBURG, VA. 24061

Mr. Anya Nagarkar
Material Sciences Corp.
Blue Bell Office Campus
Blue Bell, PA. 19422

NASA Scientific & Technical
Information Facility
P.O. Box 8757
Baltimore/Washington Inter. Air.
Baltimore, MD. 21240

Newman Library - VPI&SU

Mr. David A. O'Brien
5902 Kingsford Pl.
Bethesda, MD 20034

Dr. Donald W. Oplinger
Army Materials & Mechanics
Research Center
Department of the Army
Watertown, MA. 02171

Dr. Nicholas J. Pagano
WPAFB/MBM
Wright Patterson AFB
Ohio 45433

Dr. Nicholas Perrone, Director
Structural Mechanics Program
Department of the Navy
Office of Naval Research
Arlington, VA. 22217

Prof. T. H. H. Pian
Mass. Inst. of Tech.
Dept. of Aero. & Astr.
Cambridge, MA. 02139

Mr. Marek-Jerzy Pindera
Mail Stop 188A
NASA-Langley Research Center
Hampton, VA. 23665

Dr. R. Byron Pipes
Dept. of Mech. & Aero. Engr.
107 Evans Hall
University of Delaware
Newark, DE. 19711

Dr. K. L. Reifsnider
ESM Dept.
VPI&SU
Blacksburg, VA. 24061

Dr. Gary D. Renieri
McDonnell Douglas Astro. Co-East
P.O. Box 516
Bldg. 106, Level 4, Post C-5
St. Louis, MO. 63166

Dr. Michael W. Renieri
McDonnell Aircraft Co.
Bldg. 34, Post 350
St. Louis, MO. 63166

Dr. Larry Roderick
Mail Stop 188E
NASA-Langley Research Center
Hampton, VA. 23665

Dr. B. W. Rosen
Materials Science Corporation
Blue Bell Office Campus
Blue Bell, PA. 19422

Dr. R. E. Rowlands
Dept. of Engineering Mechanics
University of Wisconsin
Madison, WI. 53706

Dr. Edmund F. Rybicki
Battelle
Columbus Laboratories
505 King Avenue
Columbus, OH. 43201

Mr. Harminder Saluja
Boeing Vertol Company
Structural Technology
P.O. Box 16858
Philadelphia, PA. 19142

Dr. J. Wayne Sawyer
Mail Stop 190
NASA-Langley Research Center
Hampton, VA. 23665

Dr. George P. Sendeckyj
Structures Division
Air Force Flight Dynamics Lab.
Wright-Patterson AFB
Ohio 45433

Mr. Mark J. Shuart
Mail Stop 188
NASA-Langley Research Center
Hampton, VA. 23665

Dr. James H. Starnes, Jr.
Mail Stop 190
NASA-Langley Research Center
Hampton, VA. 23665

Prof. Yehuda Stavsky
Gerard Swope Prof. of Mech.
Technion-Israel Inst. of Tech.
Technion City, Haifa, Israel

Dr. W. W. Stinchcomb
ESM Dept.
VPI&SU
Blacksburg, VA. 24061

Dr. Darrel R. Tenney
Mail Code 188B
MD-Materials Research Branch
Langley Research Center
Hampton, VA. 23665

Dr. S. W. Tsai
Nonmetallic Materials Division
Air Force Materials Laboratory
Wright-Patterson AFB
Ohio 45433

Dr. J. R. Vinson
6242 Urey Hall
Applied Mechanics & Science Dept
Univ. of California-San Diego
La Jolla, CA. 92037

Mr. M. E. Waddoups
General Dynamic Corp.
Fort Worth, TX 76101

Dr. T. A. Weisshaar
Aero & Ocean Engr. Dept.
VPI&SU
Blacksburg, VA. 24061

Dr. J. M. Whitney
Nonmetallic Materials Division
Air Force Materials Laboratory
Wright-Patterson AFB
Ohio 45433

Mr. Thomas A. Zeiler
Mail Stop 395
NASA-Langley Research Center
Hampton, VA. 23665

Dr. Carl H. Zweben
General Electric Co.
Space Division
P.O. Box 8555
Philadelphia, PA. 19101

End of Document